Kidney International, Vol. 50 (1996), pp. 135–147

High resolution localization of endothelin receptors in rat renal medulla

TOKIHITO YUKIMURA, MITSURU NOTOYA, KENJI MIZOJIRI, VINCI MIZUHIRA, TAKESHI MATSUURA, TSUNEYUKI EBARA, KATSUYUKI MIURA, SHOKEI KIM, HIROSHI IWAO, and KEIFU SONG

Department of Pharmacology, Osaka City University Medical School; Developmental Research Laboratories, Shionogi & Co., Ltd.; and Department of Pharmacology, Osaka Medical College, Osaka, Japan

High resolution localization of endothelin receptors in rat renal medulla. The cellular localization of endothelin receptors in the inner medulla of the rat kidney was investigated by using high resolution light and electron microscopic autoradiography, with the microwave irradiation fixation methods. Kidney slices were incubated with ^{125}I-endothelin-1 alone or with selective ligands for the endothelin ET_B and/or ET_A receptors for light microscopic autoradiography. At the microscopic level, ^{125}I-endothelin-1 was found to bind specifically to the glomeruli, arterioles and peritubular spaces in the cortex and vasa recta and surrounding tissues in the inner medulla. These bindings were also observed when the tissue slices were incubated in the presence of IRL1620 (ET_B receptor agonist) or 97-139 (ET_A receptor antagonist). Electron microscopic autoradiography using ^{125}I-endothelin-1 in the inner medulla revealed silver grains over endothelial cells of the vasa recta and interstitial and collecting duct cells. No grains were detected over inner lining cells of the thin limbs of Henle's loop. These interstitial cells contained abundant microorganelles and lipid droplets, and had extensive cytoplasmic processes that closely related to the basement membranes of the vasa recta and loop of Henle. These findings demonstrate that type 1 interstitial cells are also primary sites for endothelin receptors as well as endothelial cells of the vasa recta and collecting duct cells in the inner medulla.

The renal medulla plays a fundamental role in maintaining body fluid and electrolyte homeostasis through medullary circulation and urine concentration [1–9]. Endothelin-1, originally identified as the most potent and long acting constrictor peptide of vascular smooth muscle [10, 11], has been implicated in regulating these processes. A high concentration of endothelin-1 decreased renal plasma flow and glomerular filtration rate in parallel in isolated perfused rat kidneys [12], in anesthetized rats [13, 14], and in humans [15], and markedly reduced urinary sodium excretion [15–18]; direct intrarenal infusion of endothelin-1 reduces medullary blood flow [19]. These effects are consistent with the vasoconstrictor action of high dose endothelin on the isolated renal artery *in vitro* [10, 20]. Recently, Rabelink et al demonstrated that endothelin-1 may have physiological and pathophysiological relevance in volume homeostasis in humans by inducing both renal vasoconstriction and sodium retention [15]. These studies suggest that endothelins may modulate the counter current system and urinary concentrating mechanisms by their actions on renal medullary circulation.

A renal vasodilator response to low dose of endothelin has been demonstrated in anesthetized cats [21], rats [22] and dogs [23]. Harris et al demonstrated that endothelin, at a low concentration, causes renal vasodilation with concomitant natriuresis due to reduced sodium transport in proximal and distal nephron segments [24]. Intrarenal arterial infusion of endothelin-1 caused enhanced renal secretion rates of prostaglandin E_2 and I_2, associated with a transient increase followed by a sustained decrease in renal blood flow [23, 25]. Endothelin-1 stimulates renal prostaglandin production in the cultured interstitial cells [26] and in the isolated inner medullary collecting duct [27]. Our previous study has shown that endothelin-3, when given into the renal artery, increased renal blood flow with no change in the systemic blood pressure. Renal vasodilation induced by endothelin-3 or IRL1620, ET_B receptor agonist, was abolished by the pretreatment with ibuprofen, a cyclooxygenase inhibitor and/or L-N^G-nitro-arginine, a nitric oxide synthase inhibitor [28, 29]. Endothelin-3 and IRL1620 increased urine flow and decreased urine osmolality; these effects were not blocked by ibuprofen or L-N^G-nitro-arginine [28, 29]. Endothelin-1 has been shown to inhibit cAMP accumulation exerted by arginine vasopressin in the collecting duct [30–32] and to inhibit Na^+,K^+-ATPase in the inner medullary collecting duct cells *in vitro* [33].

These multiple actions of the peptides have been shown to be mediated through at least two subtypes, endothelin-1-selective endothelin ET_A and non-selective endothelin ET_B receptors [34, 35]. The presence of abundant high affinity endothelin receptors was demonstrated in the kidney using membrane fractions and macro- and microautoradiography [36, 37]. In the rat kidney, specific high-affinity binding sites for endothelin have been localized to intrarenal arterial structures and glomeruli, inner medulla, vasa recta bundles and proximal convoluted tubules [37–39]. However, in these cryosections labeled *in vitro* or the injection experiments *in vivo*, the identification of the exact binding sites is limited. In the rat kidney cortex, using electron microscopic autoradiography, Furuya et al demonstrated the abundance of endothelin receptors on the glomerular and peritubular endothelial cells and the processes of peritubular interstitial cells, following intravenous administration of synthetic endothelin-1 labeled with ^{125}I [40]. However, the cellular and intracellular localization of the endothelin receptors in the medulla, where the high density

Received for publication December 5, 1994
and in revised form January 5, 1996
Accepted for publication January 8, 1996

© 1996 by the International Society of Nephrology

of binding was reported, remained unclear. In the present experiment we undertook to elucidate first, the localization of both subtypes of the endothelin receptors in the kidney using the macro- and micro-autoradiography, and second, the binding sites of endothelin-1 at the ultrastructural level, especially in the inner medulla. We incubated the renal tissue slices with ^{125}I-endothelin-1 and processed them for light microscopic and high resolution electron microscopic autoradiography, using the microwave fixation method [41, 42].

Methods

Chemicals

^{125}I-endothelin-1 (specific activity, 2200 Ci/mmol) and ^{125}I-IRL1620 (specific activity, 2200 Ci/mmol) were obtained from New England Nuclear (Boston, MA, USA). Unlabeled ET-1 was from Peptide Institute (Mino, Japan), IRL1620, Suc-[Glu^{9},Ala^{11,15}]-endothelin-1-(8–21), an ET_B receptor agonist [43] from Ciba-Geigy (Takarazuka, Japan). The ET_A receptor antagonists, FR139317, (R)2-[(R)-2-[(S)-2-[[1-(hexahydro-1H- azepinyl)]carbonyl]amino-4-methylpentanoylamino-3-[3-(1-methyl-1H-indoyl)]propionyl]amino-3-(2-pyridyl)prorionic acid [44, 45] from Fujisawa Pharmaceutical (Osaka, Japan) and 97-139, 27-O-3-[2-(3-carboxy-acryloylamino)-5-hydroxyphenyl]-acryloyloxy myricerone [46] from Shionogi (Osaka, Japan). All other chemicals were of the highest grade available.

In vitro macroautoradiography

Male Wistar rats weighing 250 to 300 g were anesthetized with sodium pentobarbital. The left kidney was removed through a retroperitoneal flank incision and the tissue blocks were frozen in isopentane at −40°C and stored at −80°C. Frozen sections (20 μm) were cut in a cryostat at −20°C. The sections were thaw-mounted on gelatin/chromic potassium sulfate-coated slides and dried overnight in a desiccator at 4°C. Light microscopy of sections stained with a methylene blue/basic fuchsin/alcohol mixture confirmed the normal glomerular and tubular structure.

After a 15 minute preincubation in 20 mM HEPES buffer containing 135 mM NaCl and 2 mM $CaCl_2$, pH 7.4, duplicate sections were incubated for 90 minutes at room temperature with 10.5 to 12.3 pM of ^{125}I-endothelin-1, in 20 mM HEPES buffer containing 135 mM NaCl and 2 mM $CaCl_2$, 0.2% bovine serum albumin and 0.01% bacitracin, pH 7.4, with or without 10^{-6} M IRL1620. Similar sections were incubated with 7.3 to 14.6 pM of ^{125}I-IRL1620. Non-specific binding was determined using alternate sections in the presence of an excess concentration (10^{-6} M) of either unlabeled endothelin-1 or IRL1620. After incubation, the sections were transferred through four successive one-minute washes of buffer without bovine serum albumin at 0°C. The slides were then rapidly dried under a stream of cold air, placed in X-ray cassettes, and exposed to X-ray films (Fuji Photo Film, Japan) for three to four days at room temperature.

Optical density of the exposed X-ray films was quantified on a Macintosh personal computer using the public domain NIH Image program, written by W. Rasband at the U.S. National Institutes of Health. The density of the autoradiograms was calibrated in terms of radioactivity density in cpm/cm^2 and was transformed in fmol/cm^2, with reference standards carried through the procedures reported by Mendelsohn and colleagues [37, 47].

Competition studies

Under the same assay condition, consecutive 20 μm sections of the rat kidney were incubated with ^{125}I-endothelin-1 with unlabeled endothelin-1 (in the range of 10^{-6} to 10^{-11} M) in the presence or absence of IRL1620 (10^{-6} M) and/or 97-139 (10^{-6} M), in 20 mM HEPES buffer containing 135 mM NaCl and 2 mM $CaCl_2$, 0.2% bovine serum albumin and 0.01% bacitracin, pH 7.4. Similar sections were incubated with 7.3 to 14.6 pM of ^{125}I-IRL1620 with unlabeled IRL1620, in the range 10^{-6} to 10^{-10} M. The slides were dried and exposed to an X-ray film. The optical density of the exposed X-ray film was determined as mentioned above.

Light and electron microscopic autoradiography

The kidneys were removed quickly from three anesthetized rats and sliced using a scalpel into about 1 to 2 mm thick tissue blocks. Each tissue block included cortex and medulla. Five tissue blocks from each kidney were immersed in ice-cold 75 mM sodium cacodylate buffer, 2 mM $CaCl_2$, 1 mM $MgCl_2$, 3% formaldehyde, pH 7.2. After a microwave irradiation at the temperature below 15°C, as previously reported [41, 42], the tissue blocks were incubated for 90 minutes and transferred through two successive 15-minute washes of ice-cold 75 mM sodium cacodylate buffer, 2 mM $CaCl_2$, 1 mM $MgCl_2$, 7% sucrose, pH 7.2. The tissue blocks then sliced with a microslicer (DTK-3000W, Dosaka EM, Kyoto) into 50 μm thick slices. Five to eight slices obtained from each tissue block were preincubated in 70 mM Tris-maleate buffer (pH 7.2) containing 0.1% bovine serum albumin and 0.01% bacitracin for 30 minutes at room temperature.

The binding sites of membrane-bound receptors were determined with good morphological characteristics, according to the methods described previously [42, 48]. Briefly, the slices were randomly divided into five vials and incubated in the same cacodylate buffer with 0.36 nM (0.79 μCi/ml) ^{125}I-endothelin-1 either alone or with one of the following: 10^{-6} M unlabeled endothelin-1; 10^{-6} M IRL1620; 10^{-6} M 97-139 (a selective non-peptide ET_A receptor antagonist); or IRL1620 plus 97-139. Following incubation, the slices were washed twice in ice-cold Tris-maleate buffer (10 min each) and fixed in 75 mM sodium cacodylate buffer, 0.5% glutaraldehyde, 3% formaldehyde, 0.3% tannic acid, pH 6.5 at room temperature for one hour, and then washed twice in 75 mM sodium cacodylate buffer, 7% sucrose, pH 7.2 for 15 minutes. The wet wt and radioactivity of slices were measured after the same incubation conditions. The slices were dehydrated in graded ethanol, and embedded in Technovit 7100 (Kulzer, Germany) for light microscopic autoradiography. Semithin 1-μm sections were dipped in Konica NR-M_2 emulsion (Konica, Tokyo, Japan) and exposed up to 60 days. The slides were developed in Konicadol-X (Konica) for four minutes and stained with methylene blue and basic fuchsin.

For electron microscopic autoradiography, eight slices incubated with ^{125}I-endothelin alone or in the presence of 10^{-6} M unlabeled endothelin-1 as mentioned above were washed twice and post-fixed with 2% OsO_4, dehydrated in graded ethanol, and embedded in epoxy resin. Ultrathin sections of 70 nm were positioned on copper grids and stained with uranyl acetate. The grids were then coated with Ilford L-4 emulsion (Ilford, UK) and exposed at 4°C for up to 90 days. After exposure, the grids were

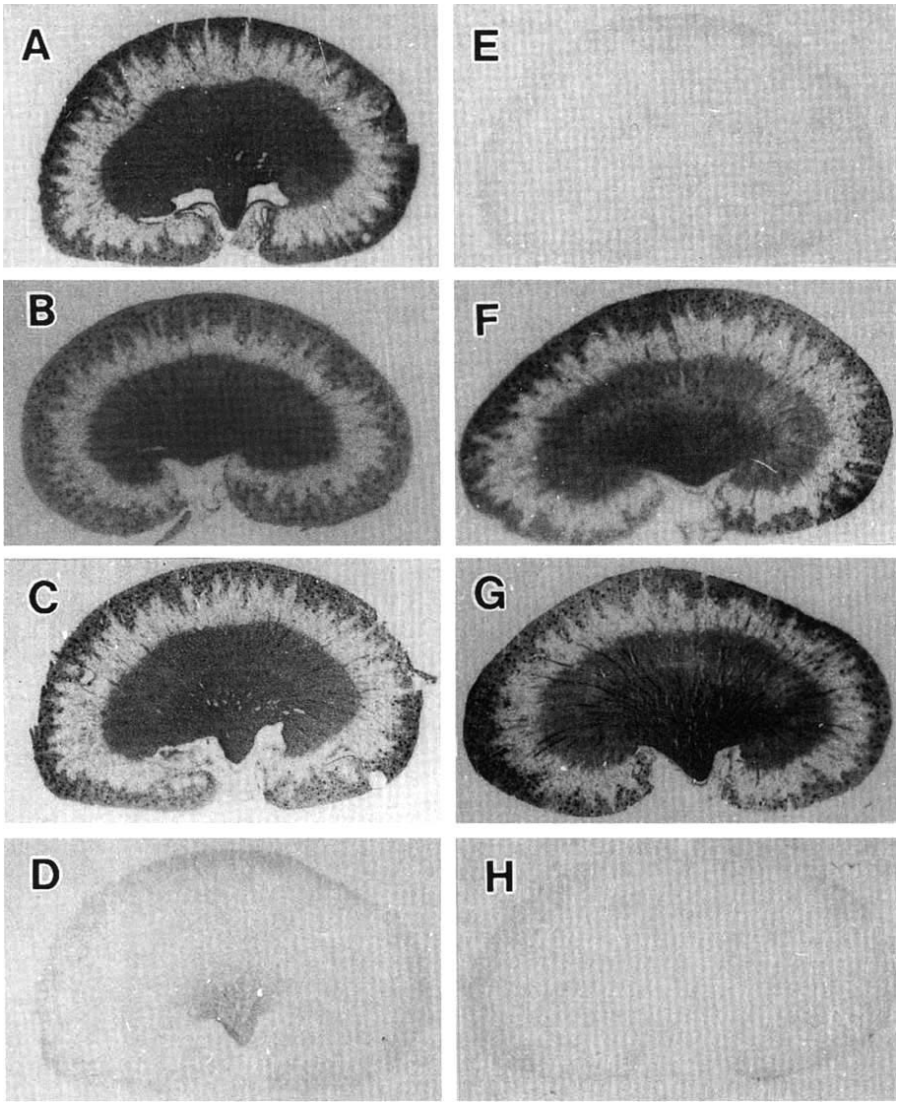

Fig. 1. *The zonal distribution of the bindings of ^{125}I-endothelin-1 (panels A, B, C, D, E) and ^{125}I-IRL1620 (panels F, G, H) in 20 μm-rat kidney sections.* **A.** The total binding of ^{125}I-endothelin-1. **B.** The bindings of with unlabeled IRL1620. **C.** The bindings with 97-139. **D.** The bindings with IRL1620 plus 97-139. **E.** Non-specific binding (the binding with unlabeled endothelin-1). **F.** The total binding of ^{125}I-IRL1620. **G.** The bindings of with FR139317. **H.** Non-specific binding (the binding with unlabeled IRL1620).

developed in Kodak Microdol-X for two minutes and the sections were examined in a JEM 1200EX electron microscope (JEOL Ltd., Tokyo, Japan).

For a careful quantitation of grain distribution in different anatomical structures, 100 electron micrographs were taken at random sampling and printed for cortex, including 52 glomeruli and 40 vessels, and 100 micrographs from the inner medulla. The number of autoradiographic grains overlying each structure was counted. The electron micrographs were scanned by a flat head scanner (GT-8000, Epson, Tokyo, Japan), and the area for each structure (number of pixels) was measured using an image processing program, the NIH Image program. Radioactivity was determined by dividing the number of grains by the area and expressed as grains per μ^2.

Statistical analysis

The results are expressed as means ± SE. Experimental data were subjected to one-way analysis of variance and significant differences were determined by Duncan's new multiple range test (SuperANOVA, Abacus Concepts, Berkeley, CA, USA). A P value smaller than 0.05 was considered to be statistically significant.

Results

Localization of renal endothelin-1 receptors by in vitro macroautoradiography

The zonal distribution of renal endothelin-1 receptors was identical to those previously reported [37, 38]. The autoradiograms representing total bindings of ^{125}I-endothelin-1 (Fig. 1A) and ^{125}I-IRL1620 (Fig. 1F) demonstrated very high densities in glomeruli in the cortex and diffuse staining throughout the inner medulla. High densities of binding occurred over longitudinal bands traversing the outer stripe of outer medulla, corresponding to vasa recta bundles, and also in the interglomerular regions and the interbundle area of the inner stripe. Binding was low in the outer stripe of the outer medulla.

A zonal distribution pattern of ^{125}I-endothelin-1 binding in the presence of excess unlabeled IRL1620 (Fig. 1B) and 97-139 (Fig. 1C), representing the ET_A and ET_B receptors, respectively, was

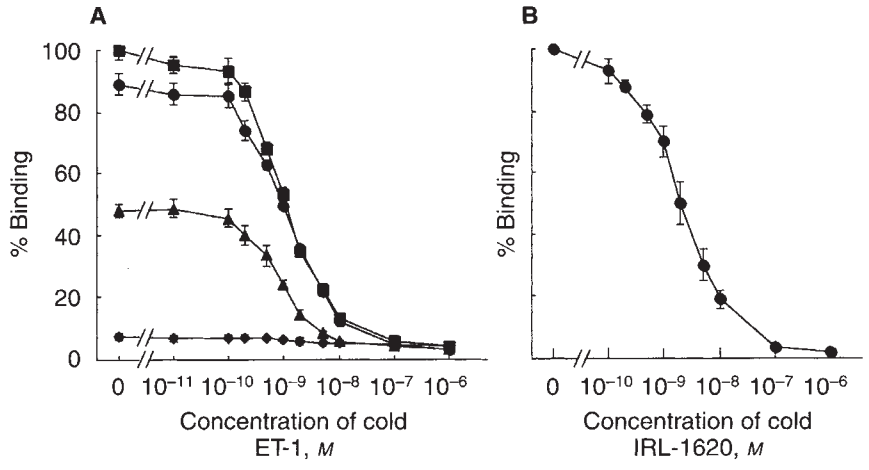

Fig. 2. *Competition curves for ^{125}I-endothelin-1 and ^{125}I-IRL1620 binding to 20 μm-rat kidney sections in the presence of increasing concentrations of unlabeled endothelin-1 (A) and IRL1620 (B), respectively.* Symbols are: (■) total; (●) with 97-139; (▲) with IRL1620; (♦) with 97-139 plus IRL1620.

identical to that of ^{125}I-endothelin-1 or ^{125}I-IRL1620 bindings (Figs. 1A and 1F). The highest density was in the inner medulla, while an intermediate density was found in the cortex and the inner stripe of the outer medulla, and low density was in the outer stripe of the outer medulla. The binding of ^{125}I-endothelin-1 that was undisplaceable by IRL1620 plus 97-139 was seen in the inner medulla, but not in the cortex and outer medulla (Fig. 1D). The relative density of binding in whole kidney and different renal areas was comparable for each case (Fig. 1). In all cases the bindings of each radioligand was almost completely abolished by excess unlabeled endothelin-1 or IRL1620, and non-specific bindings were very low, representing approximately 3% to 7% of the total binding (Fig. 1 E, H). These autoradiographic studies confirmed that both ET_A and ET_B subtypes were found throughout the renal tissue.

Quantitative autoradiography

Data from competition experiments in whole kidney sections are shown in Figure 2. Monophasic competitive inhibition curves for endothelin-1 bindings in the presence or absence of IRL1620 (ET_B agonist) or 97-139 (ET_A antagonist) revealed that each radioligand bound to an apparent single class of high affinity binding sites on sections from the rat kidney. The ET_B receptor selective ligand, IRL1620 (10^{-6} M) competed completely for the binding of ^{125}I-IRL1620 (Fig. 2) but partially for that of ^{125}I-endothelin-1. The ET_A selective 97-139 (10^{-6} M) partially but significantly competed for ^{125}I-endothelin-1 binding (Fig. 3). The total binding of ^{125}I-endothelin-1 in kidney section was 9.42 ± 0.30 fmol/cm^2. The ET_B receptor selective IRL1620 (10^{-6} M) reduced the binding to 4.50 ± 0.19 fmol/cm^2 and IRL1620 plus 97-139 to 0.70 ± 0.09 fmol/cm^2. The nonspecific binding was 0.31 ± 0.03 fmol/cm^2 (3.3% of the total binding) (Fig. 3).

Light microscopic autoradiography

The radioactivity of tissue slices after the incubation with ^{125}I-endothelin-1 alone was 7.18 ± 1.95 × 10^3 cpm/mg wet wt (Fig. 4). The non-specific binding was less than 12% of the total binding. ^{125}I-endothelin-1 penetrated into the tissue slices of the kidney and bound to the receptors. The radioactivity of slices after incubation with ET_B receptor selective IRL1620 and ET_A receptor selective 97-139 were 4.54 ± 2.12 (63.2%) and 6.92 ± 2.19 (96.4%) × 10^3 dpm/mg wet wt, respectively (Fig. 4).

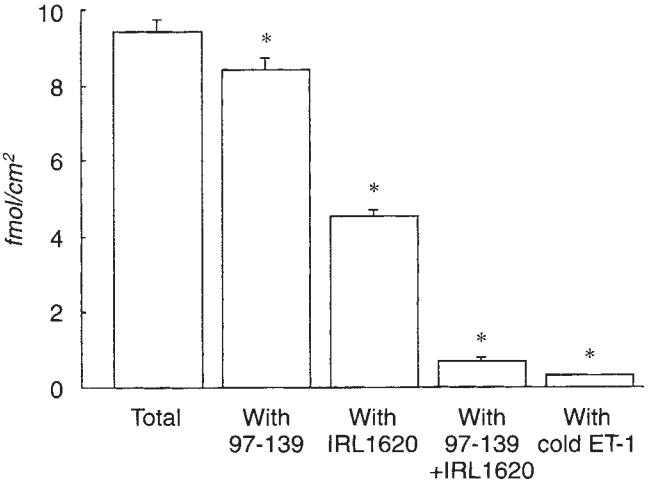

Fig. 3. *The total binding of ^{125}I-endothelin-1 in kidney sections and the binding with unlabeled 97-139 (10^{-6} M), IRL1620 (10^{-6} M), IRL1620 plus 97-139 and unlabeled endothelin-1 (10^{-6} M) in 20 μm-rat kidney sections.* The total binding of ^{125}I-endothelin-1 is 9.42 ± 0.30 fmol/cm^2. The binding was reduced by IRL1620 (10^{-6} M), IRL1620 (10^{-6} M) plus 97-139 (10^{-6} M) and unlabeled endothelin-1 (10^{-6} M). $^*P < 0.05$ the binding with IRL1620, IRL1620 plus 97-139 or unlabeled endothelin-1 versus the total binding.

By light microscopic autoradiography, silver grains were observed as dense over glomeruli and peritubular spaces but not in the tubular cells (Fig. 5). Silver grains were also observed on the endothelial and vascular smooth muscle cells of the small artery in the cortex (Fig. 5). The majority of binding was concentrated in the medulla, especially in the inner medulla, and silver grains were observed along the luminal surface of the vasa recta and over spaces surrounding the collecting duct, although detailed localization could not be determined by the light microscopic observation (Fig. 6). The binding of ^{125}I-endothelin-1 in the presence of excess unlabeled ET_B receptor selective agonist, IRL1620, presumably corresponding to the ET_A receptors, were seen in the glomeruli, small vessels and peritubular spaces in the cortex and

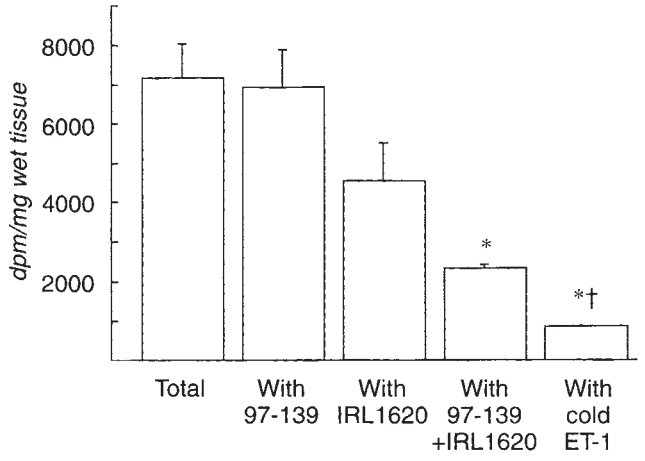

Fig. 4. *The radioactivity of tissue slices for the microautoradiography, after the incubation with ^{125}I-endothelin-1 alone or in the presence of excess concentration (10^{-6} M) of endothelin-1, IRL1620 or 97-139.* $^{*}P < 0.05$ the radioactivity with 97-139 plus IRL1620 or endothelin-1 versus the total radioactivity and the radioactivity with 97-139; $\dagger P < 0.05$ the radioactivity with endothelin-1 versus the radioactivity with IRL1620.

the inner medulla. The binding of ^{125}I-endothelin-1 undisplaceable by the ET_A receptor-selective antagonist, 97-139, was also seen in the cortex and inner medulla (ET_B receptors) (Figs. 5 C, D, and 6 C, D). The binding of ^{125}I-endothelin-1 undisplaceable by 97-139 plus IRL1620 was seen in the inner medulla (Fig. 6 G, H), but fewer binding was in the cortex (Fig. 5 G, H). These binding were almost completely abolished by unlabeled endothelin-1 (Figs. 5 I, J, and 6 I, J).

Electron microscopic autoradiography

Cortex. Silver grains were localized on the glomerular endothelial cells, not only on the thinned fenestrated endothelium as reported by Furuya et al [40], but also on the capillary endothelium adjacent to the mesangial region and on the mesangial cells (Fig. 7A). Quantified ^{125}I-endothelin-1 bindings by determining grain density over the various structures are shown in Table 1. Silver grains were sparse on the podocytes. As shown in Figure 7B and Table 1, silver grains were observed on the endothelial cells and smooth muscle cells of the small arteries surrounded by a single layer of smooth muscle cells. Silver grains were also localized on the peritubular capillary endothelial cells (Fig. 7 C, D and Table 1). Occasionally some grains were detected on the thin process of interstitial cells between the endothelial cells of peritubular capillary and tubular cells (Fig. 7C and Table 1).

Inner medulla. The grains predominantly located on the endothelial cells of the vasa recta (Fig. 8A and Table 1), and some grains were observed over the basal infoldings of the collecting duct (Fig. 8A and Table 1) and the cell body and processes of the interstitial cells (Figs. 8 A, B and Table 1) in the inner medulla. There was sparse labeling over cells of the thin loop of Henle and in the interstitial space *per se* (Table 1). The interstitial cells, in the interstitial space where banded collagen was quite evident, were type 1 interstitial cells and had multiple cytoplasmic processes in close association with the thin loop and vessels, and contained several electron-dense lipid droplets and microfilament bundles (Fig. 8).

Discussion

In the macroautoradiography, a zonal distribution pattern of ^{125}I-endothelin-1 binding in the presence of excess unlabeled IRL1620, representing the ET_A receptor, was qualitatively identical to that of ^{125}I-IRL1620 bindings representing the ET_B receptor, as shown in Figure 1. Kohzuki et al reported a similar binding profile of ^{125}I-endothelin-1, non-selective endothelin receptor ligand, and ^{125}I-sarafotoxin S6b, a selective ET_A receptor ligand in the rat kidney [37]. IRL1620 selectively blocked the binding of endothelin-1 to the ET_B receptor [43, 49], and the binding of ^{125}I-endothelin-1 to the rat kidney in the present experiment was significantly decreased by IRL1620 (Figs. 2 and 3). However, 97-139 was weak as a competing ligand for ^{125}I-endothelin-1 binding in the kidney (Figs. 3 and 4), despite a high selectivity and potent antagonism to the ET_A receptor, which was demonstrated in the *in vitro* preparations [46]. Therefore, it is suggested that the dominant subtype for endothelin receptors in the renal medulla is the ET_B receptor, as pointed out recently by others [50, 51]. Sakurai et al originally reported that isopeptide non-selective endothelin receptors (the ET_B receptors) are common in kidney, lung and brain [35]. Autoradiographic studies demonstrated dominant ET_B receptors in the human kidney, especially in the medulla [52]. The physiological importance of the ET_B receptor subtype in endothelin-induced actions in the kidney have been demonstrated in various experimental preparations by many investigators: renal vasoconstriction in rats [53], renal vasodilation and production of prostaglandins and nitric oxide in anesthetized dogs [28, 29], and stimulation of prostaglandin synthesis in cultured epithelial cells [54].

We observed the binding of ^{125}I-endothelin-1 in the inner medulla when incubated with both IRL1620 and 97-139 (Fig. 1D) that could be displaced by 10^{-6} M unlabeled endothelin-1 (Fig. 1E). There is a possibility of the presence of another receptor subtype(s) that is not an ET_A or ET_B receptor in the inner medulla.

Light microscopic autoradiograms showed that glomeruli, small vessels and peritubular spaces were heavily labeled in the kidney cortex, which were consistent with labeling experiments *in vivo* [38, 40] and *in vitro* [37, 55, 56]. Electron microscopic autoradiographic analysis revealed that ^{125}I-endothelin-1 binds to the fenestrated capillaries, peritubular capillaries and vascular endothelial and smooth muscle cells [40]. In our *in vitro* experiments, the capillary endothelium adjacent to the mesangial region and the mesangial cells were also labeled as well as the fenestrated capillaries, peritubular capillaries and vascular endothelial and smooth muscle cells, as shown in Figure 8 and Table 1. Recently, Owada et al reported that endothelin-3 enhanced cGMP production through receptor-mediated mechanism in cultured mesangial cells [57]. It was also reported that the peptide stimulated prostaglandin synthesis in cultured mesangial cells [58]. Sakamoto et al demonstrated that endothelin was synthesized by and released from cultured rat mesangial cells, and suggested the possibility that the peptide may potentially function as an autocrine factor [59].

However, Dean et al did not observe significant labeling on the glomerular mesangial cells following intravenous administration

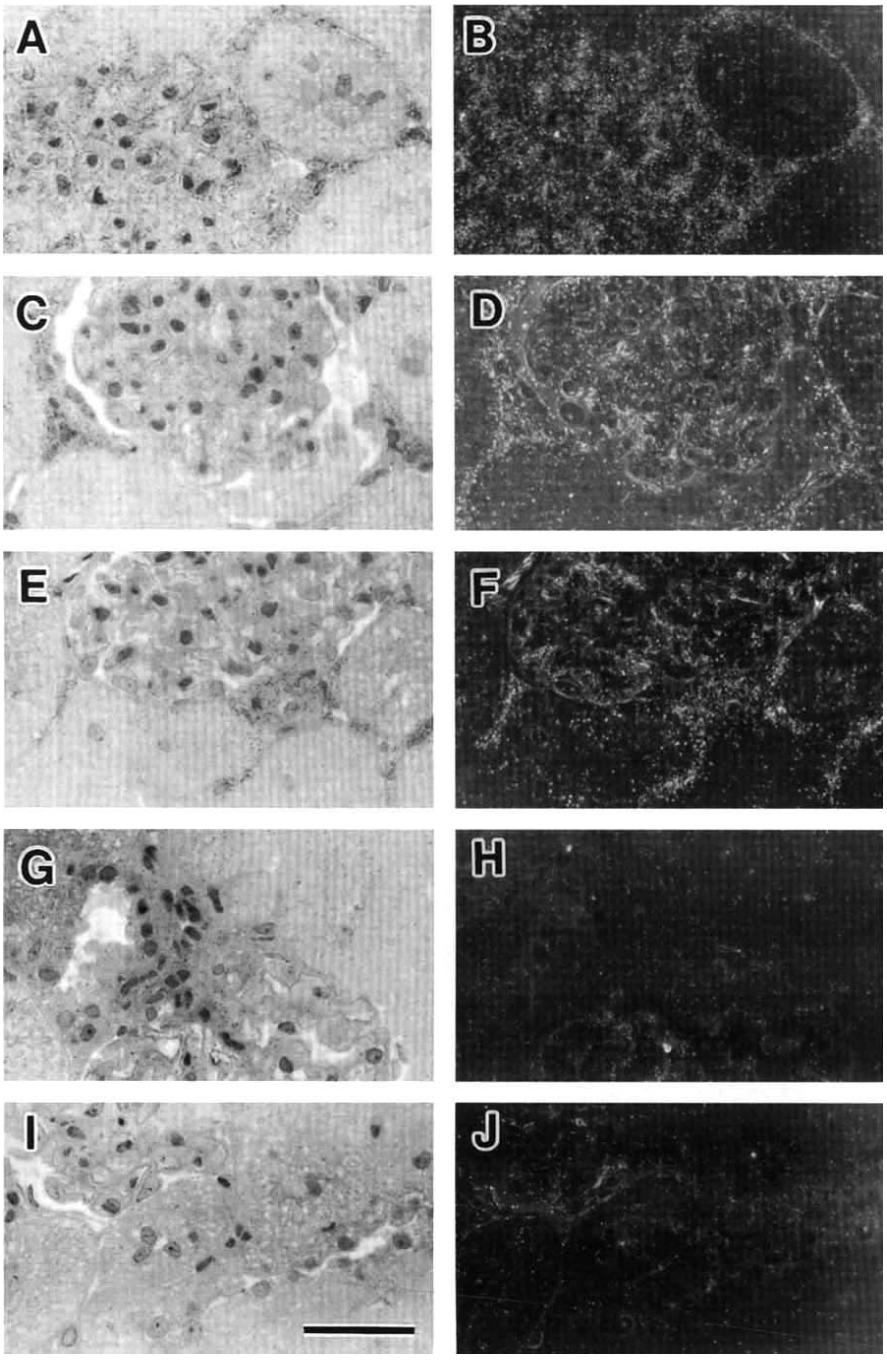

Fig. 5. *Light and dark field photos of microscopic autoradiographs of ^{125}I-endothelin-1 bindings to glomerulus, small artery and peritubular spaces in the rat kidney.* **A, B.** The total binding. **C, D.** The bindings in the presence of IRL1620. **E, F.** The bindings in the presence of 97-139. **G, H.** The bindings in the presence of IRL1620 plus 97-139. **I, J.** Non-specific binding in presence of 10^{-6} M unlabeled endothelin-1. Semi-thin 1-μm sections were dipped in Konika NR-M_2 emulsion. Bars indicate 50 μm.

of ^{125}I-endothelin-1 [60]. The differences between the reports by others [40, 60] and ours may stem from the different experimental methods used. Endogenous peptidases degrading endothelin-1 in circulating blood and in the tissues [61] or endogenous ligands for endothelin receptors, such as endothelin-1 and -3 in plasma and in the kidney, may affect the binding of the labeled peptide following intravenous injection.

The kidney medulla has a very high concentration of immunoreactive endothelin [62] and there is a significant expression of mRNA of endothelins [63–65]. Endothelin-1 was produced in these regions [62, 66]. *In situ* hybridization of both subtypes of endothelin receptors localized the gene expression of receptors in tubular cells and endothelial cells of the vasa recta [67, 68]. Endothelin-1 was reported to inhibit the activity of Na^+,K^+-ATPase [33], arginine vasopressin-stimulated cAMP accumulation and hydroosmotic response to vasopressin [30–32, 54]. Since the inner medullary collecting duct could synthesize and release the peptide, it is proposed that the peptide may have a potential role in the regulation of function of the collecting duct in an autocrine manner [27].

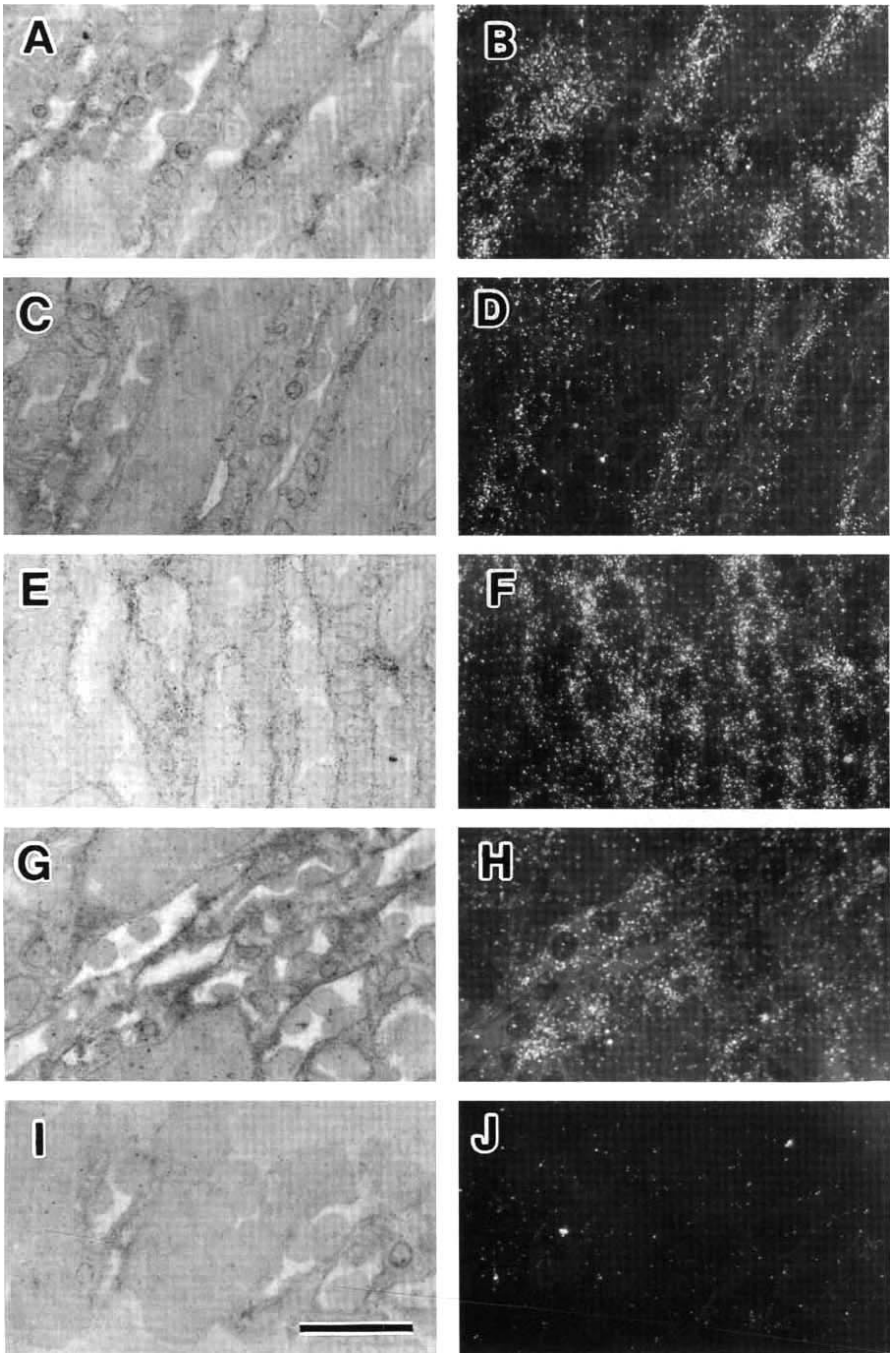

Fig. 6. *Light and dark field photos of microscopic autoradiographs of ^{125}I-endothelin-1 binding in the inner medulla of rat kidney.* **A, B.** The total binding. **C, D.** The bindings with IRL1620. **E, F.** The bindings with 97-139. **G, H.** The bindings undisplaceable by IRL1620 plus 97-139. **I, J.** The bindings were diminished in presence of 10^{-6} M unlabeled endothelin-1 (non-specific binding). Semi-thin 1-μm sections were dipped in Konika NR-M_2 emulsion. Bars indicate 50 μm.

In the present study, by using electron microscopic autoradiography, for the first time it was possible to visualize ^{125}I-endothelin-1 binding to the basal infoldings of the collecting duct cells in the inner medulla. A potential problem related to this finding would be that some of the grains over the collecting ducts may represent a source located in the endothelial cells. Indeed, our results showed that the binding density on the endothelial cells was seven times greater than that on the collecting duct cells (Table 1). However, such errors, if any, would be minor, because a wide interstitial space space exists between the basement membrane of the collecting duct cells and the adjacent endothelial cells of the vasa recta. The half distance of the autoradiography, the distance from a radioactive source that defined an area with a 50% probability of developed grain, is estimated to be far shorter than the distance between the endothelium and the collecting duct. Salpeter, McHenry and Salpeter reported that the half ditance was 0.09 μm for ^{125}I when Ilford L4 emulsion was coated on 50 to 120 nm ultrathin sections [69]. Therefore, the developed grains observed over the collecting duct cells demonstrated ^{125}I-endothelin-1 bindings to be located on the collecting duct cells

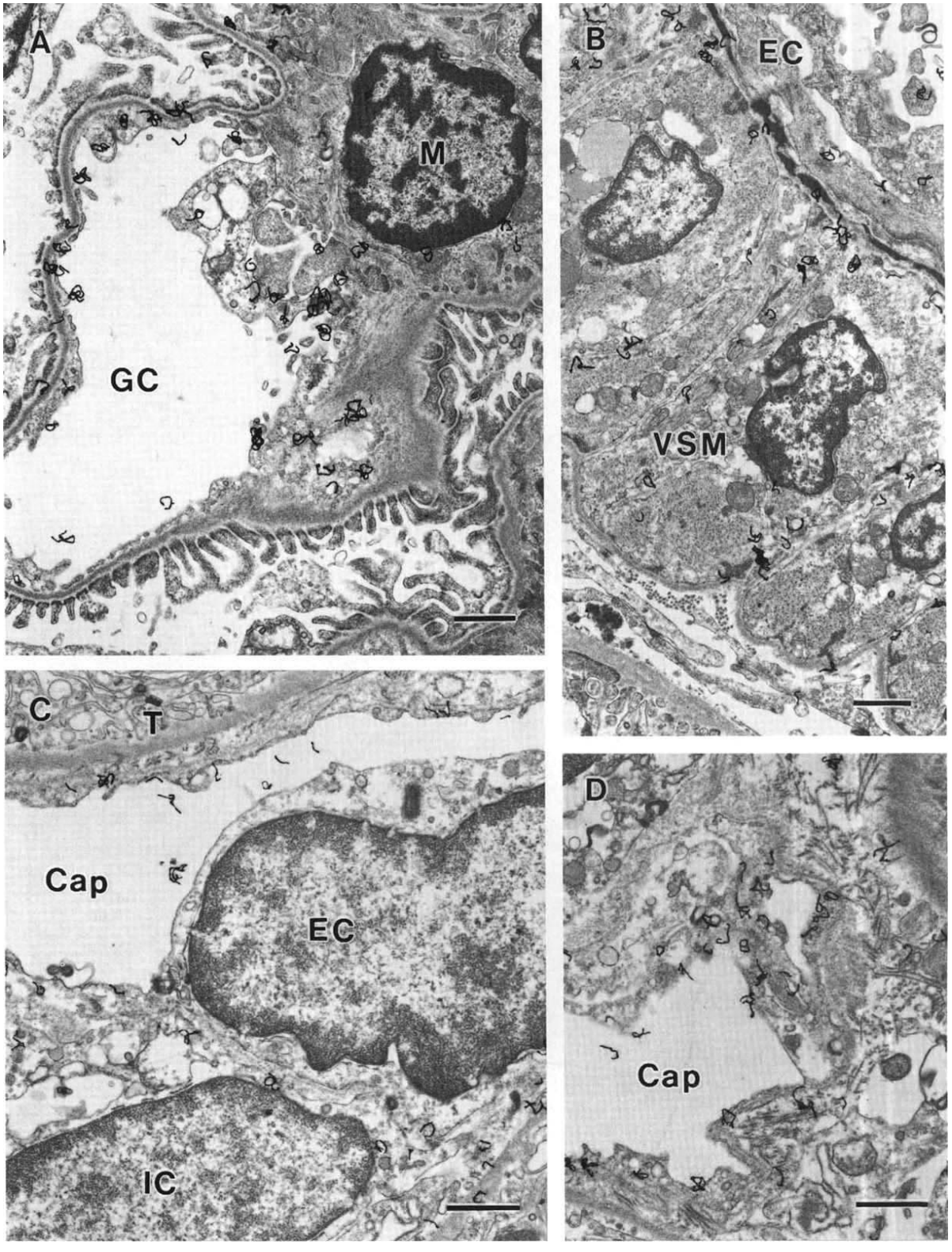

Fig. 7. *Electron microscopic autoradiographs in the rat kidney cortex.* **A.** Silver grains are located on the thinned fenestrated endothelium and the lumen near the mesangial region of the glomerular capillary (GC) and some grains are observed over the mesangial cell (M) (×5000). **B.** Silver grains are located on the endothelial cells (EC) and vascular smooth muscle cells (VSM) of the arterioles (×5000). **C** (×6000) and **D** (×6000). Silver grains on the endothelial cell (EC) of the peritubular capillary (Cap) and the thin processes of interstitial cell (IC) in the peritubular spaces. Abbreviation T is tubular cells. Bars indicate 1 μm.

Table 1. Quantitation of electron microscopic autoradiographic silver grains of specific ^{125}I-endothelin-1 binding in rat kidney cortex and inner medulla

		Grain/μ^2
Cortex		
Glomerulus	Endothelial cell	
	Cytosol	0.383
	Fenestrated	0.872
	Lumen	0.032
	Mesangial cell	0.158
	Podocyte	0.022
	Bowman space	0.002
Vasculature	Smooth muscle	0.612
	Endothelial cell	0.240
	Lumen	0.005
Tubule	Epithelial cell	0.030
	Lumen	0.004
Peritubular space		
Capillary	Endothelial cell	1.279
	Lumen	0.026
Interstitium	Interstitial cell	0.440
	Matrix	0.049
Inner medulla		
Capillary	Endothelial cell	2.922
	Lumen	0.036
Loop of Henle	Epithelial cell	0.043
	Lumen	0.011
Collecting duct	Epithelial cell	
	Basal infolding	0.405
	Cytosol	0.006
	Lumen	0.026
Interstitium	Interstitial cell	0.761
	Matrix	0.022

Electron micrographs were taken at a random sampling and printed at a final magnification of ×11,320 for cortex and inner medulla. The number of silver grains was counted and the area for each structure were determined by using the NIH image. Data are the number of grains per structure divided by the area for each structure.

and not on the endothelial cells. Therefore, our results suggest that endothelin may exert its effects directly through the receptors on the medullary collecting duct cells. Terada et al reported the presence of ET_B receptor in inner medullary collecting duct using reverse transcription-polimerase chain reaction [67], and that endothelin-1 specifically inhibited arginine vasopressin-dependent cAMP accumulation in cortical and medullary collecting ducts of the rat kidney, thereby explaining the decreased water permeability in the collecting duct and the excretion of hypotonic urine [30].

The light microscopic autoradiography with a selective ET_A receptor antagonist and an ET_B receptor agonist revealed that both ET_A and ET_B receptors exist in the inner medulla. Edwards et al [70] and Kohan, Padilla and Hughes [54] suggested that the ET_B receptor is responsible for the effects of endothelins in rat inner medullary collecting duct, although both receptor subtypes have been detected in inner medullary collecting duct cells. Although the physiological roles of the ET_A receptors remained unclear, Warner et al reported that the vasoconstriction and the prostanoids release induced by endothelin peptides are mediated by the activation of both ET_A and ET_B receptors in the isolated perfused kidney of the rat [71].

Careful fixation of specimens using tannic acid [41, 42] is feasible for high resolution localization of ^{125}I-endothelin-1 binding sites in the medulla. Localization of endothelin receptors to the interstitial cell found in the inner medulla was unexpected, although the potent actions of the peptide on the renal vascular and tubular systems were well documented. A high density of binding of endothelin-1 was observed over the inner medulla, in macro- and microautoradiography in the present experiments, and are reported in the rat and human kidney [37, 55, 72]. In the present electron microscopic autoradiography, while there is a great density of grains associated with the endothelial cells of the vasa recta, silver grains were apparently observed over the cell body and elongated cellular process of the interstitial cell, providing an additional insights in endothelin actions in the kidney. The cells in the interstitium of the inner medulla which bound to ^{125}I-endothelin-1 were identified as type 1 interstitial cells. Type 1 interstitial cells are the most abundant interstitial cells in the medulla, especially in the inner medulla, are stellate in shape with elongated cellular processes, and are characterized by the presence of numerous electron-dense lipid droplets [1, 6, 73].

The physiological significance of the existence of endothelin receptors on the type 1 interstitial cells has to be elucidated. The interstitial cells are known as major sites of renal prostaglandin production enhanced by vasoactive peptides such as angiotensin, vasopressin and bradykinin. We reported that intrarenal administration of endothelin-1 enhanced the renal secretion rate and urinary excretion of prostaglandin E_2 and I_2 in anesthetized dogs, and that renal vasodilation induced by endothelin-3 or IRL1620 via the ET_B receptor was partially antagonized in dogs treated with cyclooxygenase inhibitors [23, 28]. Using cultured rat renal medullary interstitial cells, Wilkes et al reported that endothelin-1 elevated cytosolic free calcium ion concentration with activation of phosphatidylinositol-specific phospholipase C and markedly stimulated prostaglandin E_2 production [26]. The lipid droplets contain a lot of arachidonic acid [74] and the volume density of lipid droplets, in the inner medullary interstitial cells, increased in hydrated or acutely dehydrated rats [75]. Moreover, the lipid droplets that consist mainly of triglycerides are related to the antihypertensive function of the interstitial cells, as Muirhead et al found using a transplantation experiment of renal papillary tissue [76].

Taken together, these data suggest that prostaglandin production and release in the inner medullary interstitial cells induced by endothelin peptides, like other agonists, may play a role in regulation of renal hemodynamics and urine formation.

In addition to the modulation of vascular smooth muscle tone and tubular transport, endothelin-1 exerts profound effects on the mitogenic potential and extracellular matrix formation in various mesenchymal cells [77–79]. Recent studies have revealed that endothelin-1, like angiotensin II, directly stimulates the formation of the extracellular matrix, such as fibronectin in the vascular smooth muscle [78] and collagen type I and type III in cardiac fibroblasts [79]. The binding sites of endothelin-1 were also found in the interstitial fibroblast-like cells of the cortex. However, it is still unknown whether the peptide may be involved in extracellular matrix synthesis by renal cortical interstitial cells.

A complex correlation exists between endothelins and angiotensin II; endothelin-1 increases endothelial angiotensin II production by modulating angiotensin converting enzyme activity [80]. Endothelin-1 releases from the cultured endothelial cells [81] and from the isolated aorta [82, 83] were increased by angiotensin II. It has been demonstrated that angiotensin II

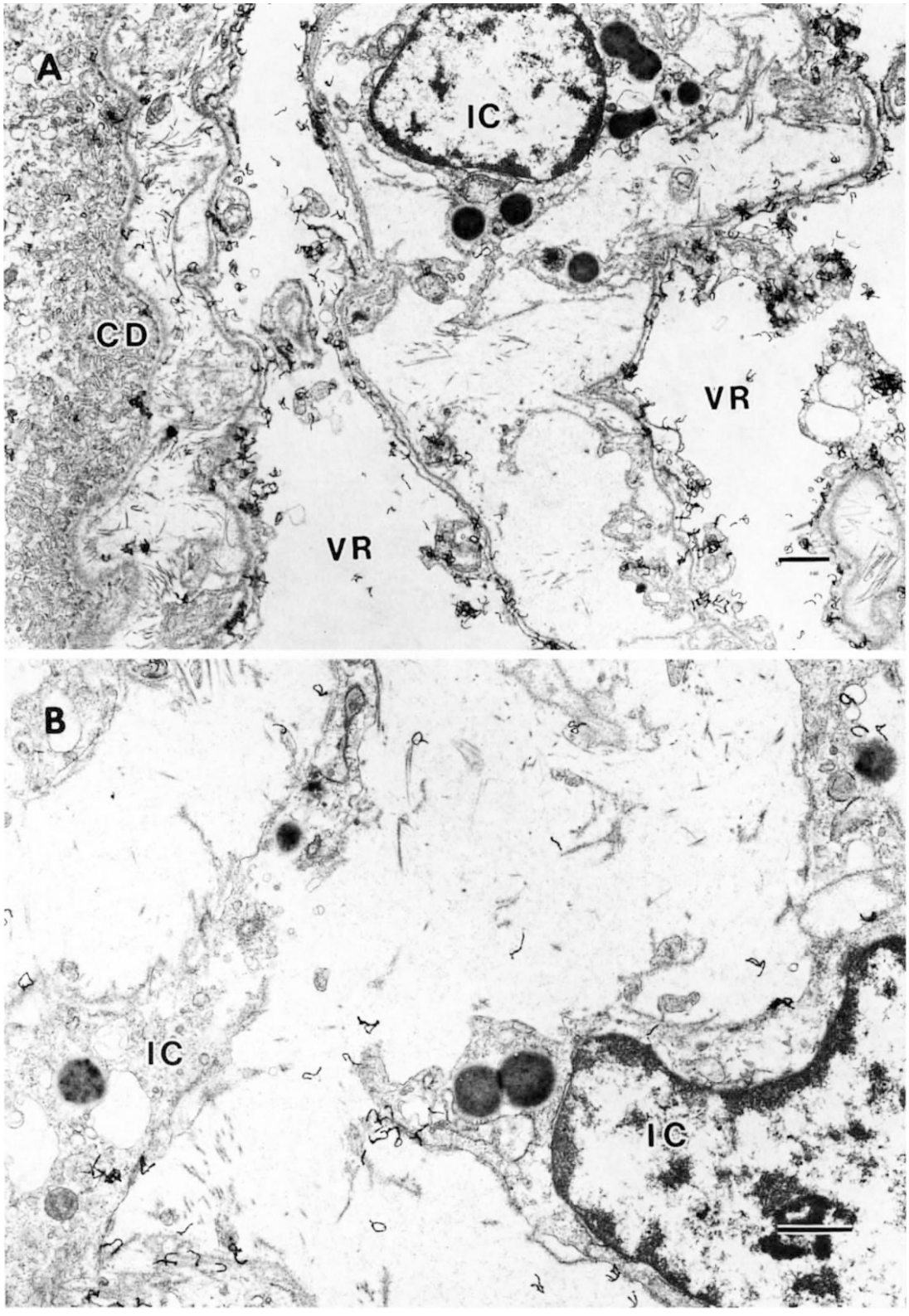

Fig. 8. *Electron microscopic autoradiographs in the inner medulla of the rat kidney are shown in* **A** *(×3000) and* **B** *(×3000).* The grains are predominantly located on the endothelial cells of the vasa recta (VR), the basal infoldings of the collecting duct cells (CD) and the stellate type 1 interstitial cells (IC) with multiple cytoplasmic processes, containing several electron-dense lipid droplets and microfilament bundles. Bars indicate 1 μm.

increases endothelin mRNA expression in cultured human vascular smooth muscle cells, and these effects of angiotensin II are suppressed by the specific receptor antagonist [84]. Endothelin-1 and angiotensin II were reported to work synergistically in the regulation of blood pressure [85] and vascular tonicity [86]. Interestingly, type 1 interstitial cells in the inner stripe of outer medulla are the primary sites for a high density of angiotensin II receptors, but not in the inner medulla [6]. The different distribution of angiotensin II and endothelin receptors in the medulla raises the possibility that both peptides may synergistically affect the medullary functions in different regions, that is, in the outer and inner medulla, respectively.

In summary, the present findings indicate that the endothelial cells of vasa recta are major sites for endothelin receptors. Endothelin receptors located in the type 1 interstitial cells and collecting duct cells suggest that intrarenal or circulating endothelin may interact with these cells to modulate medullary circulation, urine formation and the structure of the renal medulla.

Reprint requests to Tokihito Yukimura, M.D., Department of Pharmacology, Osaka City University Medical School, Asahimachi 1-4-54, Abeno-ku, Osaka 545, Japan.

References

1. KRIZ W: Structural organization of renal medullary circulation. *Nephron* 31:290–295, 1982
2. BOUBY N, TRINH-TRANG-TAN MM, DOUTE M, BANKIR L: Effects of osmolality and antidiuretic hormone on prostaglandin synthesis by renal papilla. Study in Brattleboro rats with diabetes insipidus. *Pflügers Arch* 400:96–99, 1984
3. LEMLEY KV, KRIZ W: Anatomy of the renal interstitium. *Kidney Int* 39:370–381, 1991
4. ZIMMERHACKL B, ROBERTSON CR, JAMISON RL: The microcirculation of the renal medulla. *Circ Res* 57:657–667, 1985
5. TEITELBAUM I: Hormone signaling systems in inner medullary collecting ducts. *Am J Physiol* 263:F985–F990, 1992
6. ZHUO J, ALCORN D, ALLEN AM, MENDELSOHN FA: High resolution localization of angiotensin II receptors in rat renal medulla. *Kidney Int* 42:1372–1380, 1992
7. ZEIDEL ML: Hormonal regulation of inner medullary collecting duct sodium transport. *Am J Physiol* 265:F159–F173, 1993
8. LU SH, MATTSON DL, COWLEY AW: Renal medullary captopril delivery lowers blood pressure in spontaneously hypertensive rats. *Hypertension* 23:337–345, 1994
9. COWLEY AW, ROMAN RJ, FENOY FJ, MATTSON DL: Effect of renal medullary circulation on arterial pressure. *J Hypertens* 10(Suppl 7):S187–S193, 1992
10. YANAGISAWA M, KURIHARA H, KIMURA S, TOMOBE Y, KOBAYASHI M, MITSUI Y, YAZAKI Y, GOTO K, MASAKI T: A novel potent vasoconstrictor peptide produced by vascular endothelial cells. *Nature* 332: 411–415, 1988
11. YANAGISAWA M, INOUE A, ISHIKAWA T, KASUYA Y, KIMURA S, KUMAGAYE S, NAKAJIMA K, WATANABE TX, SAKAKIBARA S, GOTO K, MASAKI T: Primary structure, synthesis, and biological activity of rat endothelin, an endothelium-derived vasoconstrictor peptide. *Proc Natl Acad Sci USA* 85:6964–6967, 1988
12. FIRTH JD, RATCLIFFE PJ, RAINE AE, LEDINGHAM JG: Endothelin: An important factor in acute renal failure? *Lancet* 2:1179–1182, 1988
13. HIRATA Y, MATSUOKA H, KIMURA K, FUKUI K, HAYAKAWA H, SUZUKI E, SUGIMOTO T, SUGIMOTO T, YANAGISAWA M, MASAKI T: Renal vasoconstriction by the endothelial cell-derived peptide endothelin in spontaneously hypertensive rats. *Circ Res* 65:1370–1379, 1989
14. LOPEZ-FARRE A, MONTANES I, MILLAS I, LOPEZ-NOVOA JM: Effect of endothelin on renal function in rats. *Eur J Pharmacol* 163:187–189, 1989
15. RABELINK TJ, KAASJAGER KA, BOER P, STROES EG, BRAAM B, KOOMANS HA: Effects of endothelin-1 on renal function in humans: Implications for physiology and pathophysiology. *Kidney Int* 46:376–381, 1994
16. GOETZ KL, WANG BC, MADWED JB, ZHU JL, LEADLEY RJJ: Cardiovascular, renal, and endocrine responses to intravenous endothelin in conscious dogs. *Am J Physiol* 255:R1064–R1068, 1988
17. MILLER WL, REDFIELD MM, BURNETT JCJ: Integrated cardiac, renal, and endocrine actions of endothelin. *J Clin Invest* 83:317–320, 1989
18. MIURA K, YUKIMURA T, YAMASHITA Y, SHICHINO K, SHIMMEN T, SAITO M, OKUMURA M, IMANISHI M, YAMANAKA S, YAMAMOTO K: Effects of endothelin on renal hemodynamics and renal function in anesthetized dogs. *Am J Hypertens* 3:632–634, 1990
19. TSUCHIYA K, NARUSE M, SANAKA T, NARUSE K, NITTA K, DEMURA H, SUGINO N: Effects of endothelin on renal regional blood flow in dogs. *Eur J Pharmacol* 166:541–543, 1989
20. TOMOBE Y, MIYAUCHI T, SAITO A, YANAGISAWA M, KIMURA S, GOTO K, MASAKI T: Effects of endothelin on the renal artery from spontaneously hypertensive and Wistar Kyoto rats. *Eur J Pharmacol* 152:373–374, 1988
21. LIPPTON H, GOFF J, HYMAN A: Effects of endothelin in the systemic and renal vascular beds in vivo. *Eur J Pharmacol* 155:197–199, 1988
22. WRIGHT CE, FOZARD JR: Regional vasodilation is a prominent feature of the haemodynamic response to endothelin in anaesthetized, spontaneously hypertensive rats. *Eur J Pharmacol* 155:201–203, 1988
23. MIURA K, YUKIMURA T, YAMASHITA Y, SHIMMEN T, OKUMURA M, YAMANAKA S, IMANISHI M, YAMAMOTO K: Renal and femoral vascular responses to endothelin-1 in dogs: Role of prostaglandins. *J Pharmacol Exp Ther* 256:11–17, 1991
24. HARRIS PJ, ZHUO J, MENDELSOHN FA, SKINNER SL: Haemodynamic and renal tubular effects of low doses of endothelin in anaesthetized rats. *J Physiol* (Lond) 433:25–39, 1991
25. MIURA K, YUKIMURA T, YAMASHITA Y, SHIMMEN T, OKUMURA M, IMANISHI M, YAMAMOTO K: Endothelin stimulates the renal production of prostaglandin E_2 and I_2 in anesthetized dogs. *Eur J Pharmacol* 170:91–93, 1989
26. WILKES BM, RUSTON AS, MENTO P, GIRARDI E, HART D, VANDER-MOLEN M, BARNETT R, NORD EP: Characterization of endothelin 1 receptor and signal transduction mechanisms in rat medullary interstitial cells. *Am J Physiol* 260:F579–F589, 1991
27. KOHAN DE, PADILLA E: Endothelin-1 is an autocrine factor in rat inner medullary collecting ducts. *Am J Physiol* 263:F607–F612, 1992
28. YAMASHITA Y, YUKIMURA T, MIURA K, OKUMURA M, YAMAMOTO K: Effects of endothelin-3 on renal functions. *J Pharmacol Exp Ther* 259:1256–1260, 1991
29. YUKIMURA T, YAMASHITA Y, MIURA K, KIM S, IWAO H, TAKAI M, OKADA T: Renal vasodilating and diuretic actions of a selective endothelin ET_B receptor agonist, IRL1620. *Eur J Pharmacol* 264:399–405, 1994
30. TOMITA K, NONOGUCHI H, MARUMO F: Effects of endothelin on peptide-dependent cyclic adenosine monophosphate accumulation along the nephron segments of the rat. *J Clin Invest* 85:2014–2018, 1990
31. OISHI R, NONOGUCHI H, TOMITA K, MARUMO F: Endothelin-1 inhibits AVP-stimulated osmotic water permeability in rat inner medullary collecting duct. *Am J Physiol* 261:F951–F956, 1991
32. NADLER SP, ZIMPELMANN JA, HEBERT RL: Endothelin inhibits vasopressin-stimulated water permeability in rat terminal inner medullary collecting duct. *J Clin Invest* 90:1458–1466, 1992
33. ZEIDEL ML, BRADY HR, KONE BC, GULLANS SR, BRENNER BM: Endothelin, a peptide inhibitor of Na^+,K^+-ATPase in intact renal tubular epithelial cells. *Am J Physiol* 257:C1101–C1107, 1989
34. ARAI H, HORI S, ARAMORI I, OHKUBO H, NAKANISHI S: Cloning and expression of a cDNA encoding an endothelin receptor. *Nature* 348:730–732, 1990
35. SAKURAI T, YANAGISAWA M, TAKUWA Y, MIYAZAKI H, KIMURA S, GOTO K, MASAKI T: Cloning of a cDNA encoding a non-isopeptide-selective subtype of the endothelin receptor. *Nature* 348:732–735, 1990
36. MARTIN ER, MARSDEN PA, BRENNER BM, BALLERMANN BJ: Identification and characterization of endothelin binding sites in rat renal papillary and glomerular membranes. *Biochem Biophys Res Commun* 162:130–137, 1989
37. KOHZUKI M, JOHNSTON CI, CHAI SY, CASLEY DJ, MENDELSOHN FA: Localization of endothelin receptors in rat kidney. *Eur J Pharmacol* 160:193–194, 1989

38. KOSEKI C, IMAI M, HIRATA Y, YANAGISAWA M, MASAKI T: Autoradiographic distribution in rat tissues of binding sites for endothelin: A neuropeptide? *Am J Physiol* 256:R858–R866, 1989
39. ORITA Y, FUJIWARA Y, OCHI S, TAKAMA T, FUKUNAGA M, YOKOYAMA K: Endothelin-1 receptors in rat renal glomeruli. *J Cardiovasc Pharmacol* 13(Suppl 5):S159–S161, 1989
40. FURUYA S, NARUSE S, NAKAYAMA T, NOKIHARA K: Effect and distribution of intravenously injected ^{125}I-endothelin-1 in rat kidney and lung examined by electron microscopic radioautography. *Anat Embryol* (Berlin) 185:87–96, 1992
41. MIZUHIRA V, HASEGAWA H, NOTOYA M: Microwave fixation method for histo- and cytochemistry, in *Electron Microscopic Cytochemistry and Immunocytochemistry in Biomedicine*, edited by OGAWA K, BARKA T, Boca Raton, CRC Press, 1993, pp 17–27
42. MIZUHIRA V, NOTOYA M, HASEGAWA H: Demonstration of steroid and peptide hormone receptors by electron microscope autoradiography, in *Autoradiography and Correlative Imaging*, edited by STUMPF WE, SAR M, San Diego, Academic Press, 1995, pp 497–513
43. TAKAI M, UMEMURA I, YAMASAKI K, WATAKABE T, FUJITANI Y, ODA K, URADE Y, INUI T, YAMAMURA T, OKADA T: A potent and specific agonist, Suc-[Glu^{9},Ala^{11,15}]-endothelin-1(8–21), IRL 1620, for the ET_B receptor. *Biochem Biophys Res Commun* 184:953–959, 1992
44. ARAMORI I, NIREI H, SHOUBO M, SOGABE K, NAKAMURA K, KOJO H, NOTSU Y, ONO T, NAKANISHI S: Subtype selectivity of a novel endothelin antagonist, FR139317, for the two endothelin receptors in transfected Chinese hamster ovary cells. *Mol Pharmacol* 43:127–131, 1993
45. SOGABE K, NIREI H, SHOUBO M, NOMOTO A, AO S, NOTSU Y, ONO T: Pharmacological profile of FR139317, a novel, potent endothelin ET_A receptor antagonist. *J Pharmacol Exp Ther* 264:1040–1046, 1993
46. MIHARA S, NAKAJIMA S, MATUMURA S, KOHNOIKE T, FUJIMOTO M: Pharmacological characterization of a potent nonpeptide endothelin receptor antagonist, 97-139. *J Pharmacol Exp Ther* 268:1122–1128, 1994
47. MENDELSOHN FA, ALLEN AM, CHAI SY, SEXTON PM, FIGDOR R: Overlapping distributions of receptors for atrial natriuretic peptide and angiotensin II visualized by in vitro autoradiography: Morphological basis of physiological antagonism. *Can J Physiol Pharmacol* 65:1517–1521, 1987
48. MIZUHIRA V, YOKOFUJITA J, SUZUKI H, SUGIURA Y: Demonstration of membrane-bound receptors by means of autoradiography. *Acta Histochem Cytochem* 19:687–700, 1986
49. NAMBI P, PULLEN M, SPIELMAN W: Species differences in the binding characteristics of [^{125}I]IRL-1620, a potent agonist specific for endothelin-B receptors. *J Pharmacol Exp Ther* 268:202–207, 1994
50. ROUBERT P, GILLARDROUBERT V, POURMARIN L, CORNET S, GUILMARD C, PLAS P, PIROTZKY E, CHABRIER PE, BRAQUET P: Endothelin receptor subtypes A and B are up-regulated in an experimental model of acute renal failure. *Mol Pharmacol* 45:182–188, 1994
51. BROOKS DP, DEPALMA PD, PULLEN M, NAMBI P: Characterization of canine renal endothelin receptor subtypes and their function. *J Pharmacol Exp Ther* 268:1091–1097, 1994
52. KOHZUKI M, JOHNSTON CI, ABE K, CHAI SY, CASLEY DJ, YASUJIMA M, YOSHINAGA K, MENDELSOHN FA: In vitro autoradiographic endothelin-1 binding sites and sarafotoxin S6B binding sites in rat tissues. *Clin Exp Pharmacol Physiol* 18:509–515, 1991
53. CRISTOL JP, WARNER TD, THIEMERMANN C, VANE JR: Mediation via different receptors of the vasoconstrictor effects of endothelins and sarafotoxins in the systemic circulation and renal vasculature of the anaesthetized rat. *Br J Pharmacol* 108:776–779, 1993
54. KOHAN DE, PADILLA E, HUGHES AK: Endothelin B receptor mediates ET-1 effects on cAMP and PGE_2 accumulation in rat IMCD. *Am J Physiol* 265:F670–F676, 1993
55. JONES CR, HILEY CR, PELTON JT, MILLER RC: Autoradiographic localisation of endothelin binding sites in kidney. *Eur J Pharmacol* 163:379–382, 1989
56. DAVENPORT AP, NUNEZ DJ, HALL JA, KAUMANN AJ, BROWN MJ: Autoradiographical localization of binding sites for porcine [^{125}I]endothelin-1 in humans, pigs, and rats: Functional relevance in humans. *J Cardiovasc Pharmacol* 13(Suppl 5):S166–S170, 1989
57. OWADA A, TOMITA K, TERADA Y, SAKAMOTO H, NONOGUCHI H, MARUMO F: Endothelin (ET)-3 stimulates cyclic guanosine 3′,5′-monophosphate production via ET_B receptor by producing nitric oxide in isolated rat glomerulus, and in cultured rat mesangial cells. *J Clin Invest* 93:556–563, 1994
58. KESTER M, CORONEOS E, THOMAS PJ, DUNN MJ: Endothelin stimulates prostaglandin endoperoxide synthase-2 mRNA expression and protein synthesis through a tyrosine kinase-signaling pathway in rat mesangial cells. *J Biol Chem* 269:22574–22580, 1994
59. SAKAMOTO H, SASAKI S, HIRATA Y, IMAI T, ANDO K, IDA T, SAKURAI T, YANAGISAWA M, MASAKI T, MARUMO F: Production of endothelin-1 by rat cultured mesangial cells. *Biochem Biophys Res Commun* 169:462–468, 1990
60. DEAN R, ZHUO J, ALCORN D, CASLEY D, MENDELSOHN FA: Cellular distribution of ^{125}I-endothelin-1 binding in rat kidney following in vivo labeling. *Am J Physiol* 267:F845–F852, 1994
61. JANAS J, SITKIEWICZ D, PULAWSKA MF, WARNAWIN K, JANAS RM: Purification of endothelin-1-inactivating peptidase from the rat kidney. *J Hypertens* 12:375–382, 1994
62. KITAMURA K, TANAKA T, KATO J, OGAWA T, ETO T, TANAKA K: Immunoreactive endothelin in rat kidney inner medulla: Marked decrease in spontaneously hypertensive rats. *Biochem Biophys Res Commun* 162:38–44, 1989
63. MACCUMBER MW, ROSS CA, GLASER BM, SNYDER SH: Endothelin: Visualization of mRNAs by in situ hybridization provides evidence for local action. *Proc Natl Acad Sci USA* 86:7285–7289, 1989
64. UJIIE K, TERADA Y, NONOGUCHI H, SHINOHARA M, TOMITA K, MARUMO F: Messenger RNA expression and synthesis of endothelin-1 along rat nephron segments. *J Clin Invest* 90:1043–1048, 1992
65. CHEN M, TODD-TURLA K, WANG WH, CAO X, SMART A, BROSIUS FC, KILLEN PD, KEISER JA, BRIGGS JP, SCHNERMANN J: Endothelin-1 mRNA in glomerular and epithelial cells of kidney. *Am J Physiol* 265:F542–F550, 1993
66. HUGHES AK, CLINE RC, KOHAN DE: Alterations in renal endothelin-1 production in the spontaneously hypertensive rat. *Hypertension* 20:666–673, 1992
67. TERADA Y, TOMITA K, NONOGUCHI H, MARUMO F: Different localization of two types of endothelin receptor mRNA in microdissected rat nephron segments using reverse transcription and polymerase chain reaction assay. *J Clin Invest* 90:107–112, 1992
68. HORI S, KOMATSU Y, SHIGEMOTO R, MIZUNO N, NAKANISHI S: Distinct tissue distribution and cellular localization of two messenger ribonucleic acids encoding different subtypes of rat endothelin receptors. *Endocrinology* 130:1885–1895, 1992
69. SALPETER MM, MCHENRY FA, SALPETER EE: Resolution of electron microscope autoradiography. IV. Application to analysis of autoradiographs. *J Cell Biol* 76:127–145, 1978
70. EDWARDS RM, STACK EJ, PULLEN M, NAMBI P: Endothelin inhibits vasopressin action in rat inner medullary collecting duct via the ET_B receptor. *J Pharmacol Exp Ther* 267:1028–1033, 1993
71. WARNER TD, BATTISTINI B, ALLCOCK GH, VANE JR: Endothelin ET_A and ET_B receptors mediate vasoconstriction and prostanoid release in the isolated kidney of the rat. *Eur J Pharmacol* 250:447–453, 1993
72. GRONE HJ, LAUE A, FUCHS E: Localization and quantification of [^{125}I]-endothelin binding sites in human fetal and adult kidneys–Relevance to renal ontogeny and pathophysiology. *Klin Wochenschr* 68:758–767, 1990
73. BOHMAN SO: The ultrastructure of the rat renal medulla as observed after improved fixation methods. *J Ultrastruct Res* 47:329–360, 1974
74. TOBIAN L, O'DONNEL M: Renal prostaglandins in relation to sodium regulation and hypertension. *Fed Proc* 35:2388–2392, 1976
75. BOHMAN S-O, JENSEN PK: Morphometric studies on the lipid droplets of the interstitial cells of the renal medulla in different states of diuresis. *J Ultrastruct Res* 55:182–192, 1976
76. MUIRHEAD EE, GERMAIN GS, ARMSTRONG FB, BROOKS B, LEACH BE, BYERS LW, PITCOCK JA, BROWN P: Endocrine-type antihypertensive function of renomedullary interstitial cells. *Kidney Int* 8(Suppl 4):S271–S282, 1975
77. SIMONSON MS, WANN S, MENE P, DUBYAK GR, KESTER M, NAKAZATO Y, SEDOR JR, DUNN MJ: Endothelin stimulates phospholipase C, Na^+/H^+ exchange, c-fos expression, and mitogenesis in rat mesangial cells. *J Clin Invest* 83:708–712, 1989
78. HAHN AW, RESINK TJ, MACKIE E, SCOTT BURDEN T, BUHLER FR: Effects of peptide vasoconstrictors on vessel structure. *Am J Med* 94(Suppl 4A):13S–19S, 1993

79. GUARDA E, KATWA LC, MYERS PR, TYAGI SC, WEBER KT: Effects of endothelins on collagen turnover in cardiac fibroblasts. *Cardiovasc Res* 27:2130–2134, 1993
80. KAWAGUCHI H, SAWA H, YASUDA H: Effect of endothelin on angiotensin converting enzyme activity in cultured pulmonary artery endothelial cells. *J Hypertens* 9:171–174, 1991
81. EMORI T, HIRATA Y, OHTA K, KANNO K, EGUCHI S, IMAI T, SHICHIRI M, MARUMO F: Cellular mechanism of endothelin-1 release by angiotensin and vasopressin. *Hypertension* 18:165–170, 1991
82. BOULANGER C, LUSCHER TF: Release of endothelin from the porcine aorta. Inhibition by endothelium-derived nitric oxide. *J Clin Invest* 85:587–590, 1990
83. KOHNO M, YASUNARI K, MURAKAWA K, YOKOKAWA K, HORIO T, FUKUI T, TAKEDA T: Release of immunoreactive endothelin from porcine aortic strips. *Hypertension* 15:718–723, 1990
84. RESINK TJ, HAHN AW, SCOTT-BURDEN T, POWELL J, WEBER E, BUHLER FR: Inducible endothelin mRNA expression and peptide secretion in cultured human vascular smooth muscle cells. *Biochem Biophys Res Commun* 168:1303–1310, 1990
85. YOSHIDA K, YASUJIMA M, KOHZUKI M, TSUNODA K, KUDO K, KANAZAWA M, YABE T, ABE K, YOSHINAGA K: Chronic synergistic effect of endothelin-1 and angiotensin II on blood pressure in conscious rats. *J Cardiovasc Pharmacol* 17(Suppl 7):S514–S516, 1991
86. AUGUET M, DELAFLOTTE S, GUILLON JM, CHABRIER PE, BRAQUET P: Different regulation of vascular tone by angiotensin II and endothelin-1 in rat aorta. *Eur J Pharmacol* 196:21–27, 1991